Post-translational thioamidation of methyl-coenzyme M reductase, a key enzyme in methanogenic and methanotrophic Archaea

Dipti D. Nayak[a], Nilkamal Mahanta[b], Douglas A. Mitchell[a,b,c], William W. Metcalf[a,c]

Carl R. Woese Institute for Genomic Biology, University of Illinois, Urbana, Illinois, USA[a]; Department of Chemistry, University of Illinois, Urbana, Illinois, USA[b]; Department of Microbiology, University of Illinois, Urbana, Illinois, USA[c]

Running Head: Thioglycine modification of methyl-coenzyme M reductase

Address correspondence to:

William W. Metcalf (metcalf@illinois.edu), Department of Microbiology, 601 S. Goodwin Avenue, University of Illinois, IL 61801 Tel: 217-244-1943

Douglas A. Mitchell (douglasm@illinois.edu), Department of Chemistry, 505 S. Matthews Avenue, University of Illinois, IL 61801 Tel: 217-333-0508

16 **Abstract**

17 The enzyme methyl-coenzyme M reductase (MCR), found in strictly anaerobic
18 methanogenic and methanotrophic archaea, catalyzes a reversible reaction involved in the
19 production and consumption of the potent greenhouse gas methane. The α subunit of this
20 enzyme (McrA) contains several unusual post-translational modifications, including an
21 exceptionally rare thioamidation of glycine. Based on the presumed function of homologous
22 genes involved in the biosynthesis of thioamide-containing natural products, we hypothesized
23 that the archaeal *tfuA* and *ycaO* genes would be responsible for post-translational installation of
24 thioglycine into McrA. Mass spectrometric characterization of McrA in a Δ*ycaO-tfuA* mutant of
25 the methanogenic archaeon *Methanosarcina acetivorans* revealed the presence of glycine, rather
26 than thioglycine, supporting this hypothesis. Physiological characterization of this mutant
27 suggested a new role for the thioglycine modification in enhancing protein stability, as opposed
28 to playing a direct catalytic role. The universal conservation of this modification suggests that
29 MCR arose in a thermophilic ancestor.

Introduction

Methyl-coenzyme M reductase (MCR) is a unique enzyme found exclusively in anaerobic archaea, where it catalyzes the reversible conversion of methyl-coenzyme M (CoM, 2-methylmercaptoethanesulfonate) and coenzyme B (CoB, 7-thioheptanoylthreoninephosphate) to methane and a CoB-CoM heterodisulfide (1, 2):

$$CH_3 - S - CoM + HS - CoB \leftrightarrow CH_4 + CoM - S - S - CoB$$

This enzymatic reaction, which is believed to proceed via an unprecedented methyl radical intermediate (3), plays a critical role in the global carbon cycle (4). Thus, in the forward direction MCR catalyzes the formation of methane in methane-producing archaea (methanogens), whereas the enzyme initiates methane consumption in methanotrophic archaea (known as ANMEs for anaerobic oxidation of methane) in the reverse direction. Together, these processes produce and consume gigatons of methane each year, helping to establish the steady-state atmospheric levels of an important greenhouse gas. MCR displays an $\alpha_2\beta_2\gamma_2$ protein domain architecture and contains two molecules of a nickel-containing porphinoid cofactor, F_{430} (1, 5, 6). The reduced Ni(I) form of F_{430} is essential for catalysis (7), but is highly sensitive to oxidative inactivation, a feature that renders biochemical characterization of MCR especially challenging. As a result, many attributes of this important enzyme remain uncharacterized.

One of the most unusual features of MCR is the presence of several modified amino acids within the active site of the α-subunit. Among these are a group of methylated amino acids, including 3-methylhistidine (or N^1-methylhistidine), *S*-methylcysteine, 5(S)-methylarginine, and 2(S)-methylglutamine, which are likely installed post-translationally by *S*-adenosylmethionine-dependent methyltransferases (8, 9). 3-methylhistidine is found in all MCRs examined to date, whereas the presence of the other methylated amino acids is variable among methane-metabolizing archaea (9). A didehydroaspartate modification is also observed in some, but not all, methanogens (10). Lastly, a highly unusual thioglycine modification, in which the peptide amide bond is converted to a thioamide, is present in all methanogens that have been analyzed to date (1, 9).

The function(s) of the modified amino acids in MCR has/have not yet been experimentally addressed; however, several theories have been postulated. The 3-methylhistidine may serve to position the imidazole ring that coordinates CoB. This methylation also alters the pK_a of histidine in a manner that would promote tighter CoB-binding (11). The variable occurrence of the other methylated amino acids suggests that they are unlikely to be directly involved in catalysis. Rather, it has been hypothesized that they tune enzyme activity by altering the hydrophobicity and flexibility of the active site pocket (9, 11). A similar argument has been made for the didehydroaspartate residue (10). In contrast, two distinct mechanistic hypotheses

64 implicate the thioglycine residue in catalysis. The first proposes that thioglycine facilitates
65 deprotonation of CoB by reducing the pK_a of the sulfhydryl group (12); the second suggests that
66 thioglycine could serve as an intermediate electron carrier for oxidation of a proposed
67 heterodisulfide anion radical intermediate (13).

68 Thioamides are rare in biology. While cycasthioamide is plant-derived (14), most other
69 naturally occurring thioamides are of prokaryotic origin. Among these are the ribosomally
70 synthesized and post-translationally modified (RiPP) peptide natural products thioviridamide
71 (15) and methanobactin (16–18), as well closthioamide, which appears to be an unusual non-
72 ribosomal peptide (19, 20). The nucleotide derivatives thiouridine and thioguanine (21), and two
73 additional natural product antibiotics, thiopeptin and Sch 18640 (22, 23), also contain thioamide
74 moieties. Although the mechanism of thioamide installation has yet to be established, the recent
75 identification of the thioviridamide biosynthetic gene cluster provides clues to their origin (24).
76 Two of the proteins encoded by this gene cluster have plausible roles in thioamide synthesis. The
77 first, TvaH, is a member of the YcaO superfamily, while the second, TvaI, is annotated as a
78 "TfuA-like" protein (24). Biochemical analyses of YcaO-family proteins indicate that they
79 catalyze the ATP-dependent cyclodehydration of cysteine, serine, and threonine residues to the
80 corresponding thiazoline, oxazoline, and methyloxazoline (Fig. 1). Many azoline heterocycles
81 undergo dehydrogenation to the corresponding azole, which are prominent moieties in various

RiPP natural products classes, such as linear azol(in)e-containing peptides, thiopeptides, and cyanobactins (25–28). The YcaO-dependent synthesis of peptidic azol(in)e heterocycles often requires a partner protein, which typically is the neighboring gene in the biosynthetic cluster (29–31). Based on enzymatic similarity, the TfuA protein encoded adjacent to the YcaO in the thioviridamide pathway may also enhance the thioamidation reaction, perhaps by recruiting a sulfurtransferase protein, as reported in the biosynthesis of thiouridine and thioguanine (32, 33).

The biosynthesis of the thioglycine in MCR was proposed to occur by a mechanism similar to that used to produce thioamide-containing natural products (9), a prediction made six years prior to the discovery of the thioviridamide biosynthetic gene cluster (24). Given their putative role in thioamidation reactions, it is notable that YcaO homologs were found to be universally present in an early analysis of methanogen genomes, resulting in their designation as "methanogenesis marker protein 1" (34). Genes encoding TfuA homologs are also ubiquitous in methanogens, usually encoded in the same locus as *ycaO*, similar to their arrangement in the thioviridamide gene cluster. Therefore, both biochemical and bioinformatic evidence are consistent with these genes being involved in thioglycine biosynthesis. In this report, we use the genetically tractable methanogen *Methanosarcina acetivorans* to show that installation of the thioamide bond at Gly465 in the α-subunit of MCR requires the *ycaO-tfuA* locus. Significantly, the viability of *ycaO-tfuA* mutants precludes the hypothesis that the thioamide residue is

100 catalytically critical. Instead, our phenotypic analyses support a pivotal role for thioglycine in
101 MCR protein stability.

102 **Results**

103 **Phylogenetic analyses of TfuA and YcaO in methanogenic and methanotrophic**
104 **archaea.** To examine the possibility that YcaO and TfuA are involved in McrA thioamidation,
105 we reassessed the distribution, diversity, and phylogeny of genes encoding these proteins in
106 sequenced microbial genomes, which today comprise a much larger dataset than when
107 "methanogenesis marker protein 1" was first proposed (34). Significantly, all complete
108 methanogen and ANME genome sequences encode a YcaO homolog, with a few strains
109 encoding two copies (Fig. 2). The YcaO sequences form a distinct, well-supported clade that also
110 includes homologs from ammonia-oxidizing archaea (Fig.2 – Supplemental Figure 1). Excluding
111 the second YcaO in strains that encode two copies, the YcaO tree is congruent with the
112 phylogeny of methanogens reconstructed using housekeeping or *mcr* genes (Fig. 2). Thus, it is
113 likely that YcaO was acquired early in the evolution of methanogens and maintained largely
114 through vertical inheritance, as expected for a trait that coevolved with MCR (35, 36) .

115 TfuA homologs are encoded in the overwhelming majority of MCR-encoding taxa,
116 although a few species lack this gene. The latter include *Methanopyrus kandleri* and
117 *Methanocaldococcus janaschii*, two species previously shown to contain the thioglycine

118 modification (9) (Fig. 2). Thus, TfuA cannot be obligatorily required for thioglycine installation.
119 The archaeal TfuA proteins also fall within a single clade that is largely congruent with the
120 evolutionary history of archaea (Fig.2 – Supplemental Figure 1 and Supplemental Figure 2);
121 however, unlike YcaO, the methanogen clade includes numerous bacterial homologs (Fig.2 –
122 Supplemental Figure 2).

123 The genomic context of *tfuA* and *ycaO* in methanogens supports a shared or related
124 function, perhaps involving sulfur incorporation and/or methanogenesis (Fig. 2). When both are
125 present, the two genes comprise a single locus in which the stop codon of the upstream *ycaO*
126 gene overlaps with the start codon of the downstream *tfuA* gene, suggesting that they are co-
127 transcribed. In several instances, additional genes involved in sulfur metabolism such as *thiF*,
128 *sufS*, as well as *moaD, moaE* and *moeB* (involved in molybdopterin biosynthesis) (37, 38) are
129 found in the genomic vicinity. Occasionally, genes encoding enzymes involved in
130 methanogenesis, including the *Methanomassiliicoccus* MCR operon, are found in the
131 neighborhood (Fig. 2).

132 **TfuA and YcaO are not essential in *Methanosarcina acetivorans*.** To test their role in
133 thioglycine installation, we generated a mutant lacking the *ycaO-tfuA* locus in the genetically
134 tractable methanogen *Methanosarcina acetivorans*. Based on the hypothesis that thioglycine may
135 be imperative for MCR activity, and the knowledge that the MCR-encoding operon

(*mcrBCDAG*) is essential (39), we first examined the viability of Δ*ycaO-tfuA* mutants using a recently developed Cas9-based assay for gene essentiality (40). This assay compares the number of transformants obtained using a Cas9 gene-editing plasmid with and without a repair template that creates a gene deletion. Essential genes give similar, low numbers of transformants with or without the repair template; whereas non-essential genes give *ca*. 10^3-fold higher numbers with the repair template. Our data strongly suggest that deletion of the *ycaO-tfuA* locus has no impact on viability (Fig. 3). Several independent mutants were clonally purified and verified by PCR prior to phenotypic characterization (Figure 3 – Supplemental Figure 1).

The Δ*ycaO-tfuA* mutant lacks the McrA Gly465 thioamide. To test whether YcaO and TfuA are involved in the post-translational modification of Gly465 in McrA, we isolated the McrA protein from cell extracts of the Δ*ycaO-tfuA* mutant and its isogenic parent by excising the appropriate bands from Coomassie-stained SDS-PAGE gels. These proteins were then subjected to in-gel trypsin digestion and the resulting peptides analyzed by matrix-assisted laser desorption-ionization time-of-flight mass spectrometry (MALDI-TOF-MS). The mass spectrum of the parental strain showed a peak at *m/z* 3432 Da (Fig. 4) corresponding to the peptide ($_{461}$LGFF**G**FDLQDQCGATNVLSYQGDEGLPDELR$_{491}$) with Gly465 being thioamidated (9, 11). The identity of this peptide was confirmed by high-resolution electrospray ionization tandem MS analysis (HR-ESI-MS/MS, $[M+3H]^{3+}$ expt. *m/z* 1144.8608 Da; calc. *m/z* 1144.8546

Da; 5.4 ppm error; Fig. 4 – Supplemental Figure 1A). This peptide also contains the recently reported didehydroaspartate modification at Asp470 (10) and *S*-methylation at Cys472 (8). Consistent with the involvement of TfuA-associated YcaO proteins in thioamide formation, we noted the absence of the *m/z* 3432 Da species in the mass spectrum of a similarly treated Δ*ycaO-tfuA* sample. Instead, a predominant *m/z* 3416 Da species appeared, which was 16 Da lighter, consistent with replacement of sulfur by oxygen. HR-ESI-MS/MS analysis again confirmed the identity of this peptide as being McrA L461-R491 ($[M+3H]^{3+}$ expt. *m/z* 1139.5316 Da; calc. *m/z* 1139.5290 Da; 2.3 ppm error; Fig. 4 – Supplemental Figure 1B). In contrast to the thioglycine-containing wild-type peptide, we observed fragmentation between Gly465 and Phe466 (b_5 ion, Fig. 4 – Supplemental Figure 1B) in the Δ*ycaO-tfuA* strain. The lack of fragmentation in the wild-type peptide was anticipated based on the greater double bond character of C-N bonds in thioamides (41). The *m/z* 3375 Da species present in both samples corresponds to an unrelated tryptic peptide, McrA Asp392-Arg421 (Fig. 4 – Supplemental Figure 2). We also observed a peak at *m/z* 1496 in both the parent and mutant samples corresponding to a *N*-methylhistidine-containing tryptic peptide (His271-Arg284, Fig. 4 – Supplemental Figure 3A). Thus, thioglycine formation is not a prerequisite for this modification. Additionally, a peak observed *m/z* 1561, corresponding to McrA Phe408-Arg421, shows that Gln420 remains unmodified in *M.*

171 *acetivorans*, as has previously been observed for *Methanosarcina barkeri* (Fig. 4 – Supplemental
172 Figure 3B) (9).

173 **Growth defects associated with loss of the McrA thioglycine modification.** To
174 understand potential phenotypic consequences of losing the thioglycine modification, we
175 quantified the doubling time and growth yield by monitoring changes in optical density during
176 growth of *M. acetivorans* on a variety of substrates (Table 1). While no significant differences
177 were observed during growth on methanol or trimethylamine hydrochloride (TMA) at 36 °C, the
178 Δ*ycaO-tfuA* mutant had substantially longer generation times and lower cell yields on both
179 dimethylsulfide (DMS) and acetate (Table 1). Interestingly, the growth phenotype on methanol
180 medium was strongly temperature-dependent, with no observed differences at 29 and 36 °C, but
181 severe defects for the Δ*ycaO-tfuA* mutant at 39 and 42 °C. Unlike the parental strain, the mutant
182 was incapable of growth at 45 °C (Fig. 5).

183

184 **Discussion**

185 The loss of the thioglycine modification in the Δ*ycaO-tfuA* mutant suggests that these genes
186 are directly involved in the post-translational modification of McrA. Mechanistically, this
187 conclusion is compatible with biochemical analyses of YcaO homologs. YcaO enzymes that
188 carry out the ATP-dependent cyclodehydration of beta-nucleophile-containing amino acids have

189 been extensively investigated (28). Such cyclodehydratases coordinate the nucleophilic attack of
190 the cysteine, serine, and threonine side chain on the preceding amide carbonyl carbon in a
191 fashion reminiscent of intein splicing (42) (Fig. 1). The enzyme then *O*-phosphorylates the
192 resulting oxyanion and subsequently *N*-deprotonates the hemiorthoamide, yielding an azoline
193 heterocycle. An analogous reaction can be drawn for the YcaO-dependent formation of peptidic
194 thioamides. The only difference is that an exogenous equivalent of sulfide is required for the
195 thioamidation reaction, rather than an adjacent beta-nucleophile-containing amino acid for
196 azoline formation (Fig. 1).

197 Most YcaO cyclodehydratases require a partner protein for catalytic activity. The earliest
198 investigated YcaO partner proteins are homologs of the ThiF/MoeB family, which are related to
199 E1 ubiquitin-activating enzymes (26, 43). These YcaO partner proteins, as well as the more
200 recently characterized "ocin-ThiF" variety (30), contain a ~90-residue domain referred to as the
201 RiPP Recognition Element (RRE), which facilitates substrate recognition by interacting with the
202 leader peptide. Considering these traits of azoline-forming YcaOs, it is possible that thioamide-
203 forming YcaOs require the TfuA partner to facilitate binding to the peptidic substrate.
204 Alternatively, TfuA may recruit and deliver sulfide equivalents by a direct or indirect
205 mechanism. In this regard, it is noteworthy that the *ycaO-tfuA* locus can be found adjacent to
206 genes involved in sulfur and molybdoterin metabolism (Fig. 2). Many of these genes encode

proteins with rhodanese-like homology domains, which are well-established sulfurtransferases. These enzymes typically carry sulfur in the form of a cysteine persulfide, a non-toxic but reactive equivalent of H_2S (33, 44). Akin to rare cases of azoline-forming, partner-independent YcaOs, certain methanogens lack a bioinformatically identifiable TfuA (*e.g. Methanopyrus kandleri* and *Methanocaldococcus* sp.). Whether these proteins use an as yet unidentified protein or are truly independent sulfur insertion enzymes remains to be seen. Clearly, further *in vitro* experimentation will be required to delineate the precise role of TfuA in the thioamidation reaction.

The viability of the Δ*ycaO-tfuA* mutant raises significant questions as to the role of thioglycine in the native MCR enzyme, especially considering its universal presence in all MCRs examined to date. We considered three hypotheses to explain this result. First, as we examined the previously suggested possibility that thioglycine modification is involved in enzyme catalysis (9, 13), which would be manifest in a slower reaction rate. As MCR is thought to be the rate-limiting step of methanogenesis (2, 3), this should be reflected in a corresponding decrease in the growth rate on various substrates, with more pronounced defects on substrates that lead to the fastest growth. Significantly, we observed the exact opposite, with the most pronounced defects being observed substrates that support the slowest growth rates in wild-type cells. Thus, loss of the thioglycine modification does not affect the rate-limiting step in growth and therefore is

225 unlikely to result in a slower enzyme. Next, we considered the possibility that thioglycine
226 influences substrate affinity. If so, we expected that differences in metabolite pools caused by
227 growth on different substrates might be reflected in altered growth patterns for the mutant. In
228 particular, C_1 units enter methanogenesis at the level of N^5-methyl-tetrahydrosarcinapterin (CH_3-
229 H_4SPt) during growth on acetate, but at the level of methyl-CoM (45, 46) during growth on
230 DMS, methanol and TMA (Fig. 5 – Supplemental Figure 1; (47, 48)). Significantly, these entry
231 points are separated by an energy-dependent step that is coupled to production or consumption of
232 the cross-membrane sodium gradient. As a result, intracellular levels of methyl-CoM, CoM and
233 CoB could possibly be significantly different depending on the entry point into the methanogenic
234 pathway. Because we observed growth defects on substrates that enter at both points (*i.e.* DMS
235 and acetate), we suspect that the growth deficiency phenotype is unlikely to be related to changes
236 in substrate affinity. However, we recognize that metabolite pools are also affected by the
237 energetics of the methanogenic pathway. Indeed, the growth phenotypes were most severe for
238 DMS and acetate, which are the substrates with the lowest available free energy. The Gibbs free
239 energy ($\Delta G°'$) for methanogenesis from acetate and DMS are -36 kJ/mol CH_4 (49) and -49.2
240 kJ/mol CH_4 (50), respectively, which is considerably lower than the -102.5 kJ/mol CH_4 and -77.6
241 kJ/mol CH_4 for methanol and TMA, respectively (51). Therefore, it remains possible that
242 changes in the substrate pools are responsible for the substrate-dependent growth phenotypes. A

243 third explanation considered was that thioglycine increases the thermal stability of MCR. In this
244 model, unstable MCR protein would need to be replaced more often, creating a significant
245 metabolic burden for the mutant. Consistent with our results, this additional burden would be
246 exacerbated on lower energy substrates like DMS and acetate, especially given the fact that
247 MCR comprises *ca*. 10% of the cellular protein (52). Further, one would expect that a protein
248 stability phenotype would be exaggerated at higher temperatures, which we observed during
249 growth on methanol. Thus, multiple lines of evidence support the idea that the growth-associated
250 phenotypes stemming from the deletion of TfuA and YcaO are caused by decreased MCR
251 stability.

252 The chemical properties of amides relative to those of thioamides are consistent with our
253 thermal stability hypothesis. Although amides tend to be planar, they have a low rotational
254 barrier and are, thus, conformationally flexible. In contrast, thioamides have higher barriers to
255 rotation and also lessened preference for the *s*-cis conformation (41). Moreover, sulfur has a
256 larger van der Waals radius than oxygen resulting in a thioamide bond length that is ~40% longer
257 than the amide bond (1.71Å versus 1.23Å) (53), which presents additional steric hindrances to
258 backbone flexibility. Finally, the pK_a of thioamides is lower than the oxygen-containing
259 counterpart, making thioglycine a stronger hydrogen bond donor than glycine (54), which again
260 would reduce conformational flexibility. Taken together, it seems reasonable to conclude that the

261 increased flexibility of the unmodified glycine in the Δ*ycaO-tfuA* mutant results in a protein that
262 is prone to denaturation and enhanced rates of cellular degradation. A conclusive test of this
263 hypothesis will require comprehensive biochemical and biophysical characterization of the MCR
264 variant lacking the thioglycine modification, which is beyond the scope of this work.

265 Finally, the temperature-sensitive phenotype of the Δ*ycaO-tfuA* mutant has potential
266 implications regarding the evolution and ecology of methanogenic archaea. Based on this result,
267 it seems reasonable to speculate that the thioglycine modification would be indispensable for
268 thermophilic methanogens. It is often posited that the ancestor of modern methanogens was a
269 thermophilic organism (55–57). If so, one would expect the thioglycine modification to be
270 present in most methanogenic lineages, being stochastically lost due to genetic drift only in
271 lineages that grow at low temperatures where the modification is not required. In contrast, if
272 methanogenesis evolved in a cooler environment, one might expect the distribution of the
273 modification to be restricted to thermophilic lineages. Thus, the universal presence of the
274 thioglycine modification supports the thermophilic ancestry of methanogenesis. Indeed, the
275 *ycaO-tfuA* locus is conserved even in *Methanococcoides burtonii*, a psychrophilic methanogen
276 isolated from Ace Lake in Antarctica, where the ambient temperature is always below 2 ºC (58).
277 It will be interesting to see whether this modification is maintained by other methanogenic and
278 methanotrophic archaea growing in low temperature environments.

Materials and Methods

Bioinformatics analyses. The 1,000 closest homologs were extracted from the NCBI non-redundant protein database using the YcaO amino acid sequence (MA0165) or the TfuA amino acid sequence (MA0164) as queries in BLAST-P searches. The amino acid sequences of these proteins were aligned using the MUSCLE plug-in (59) with default parameters in Geneious version R9 (60). Approximate maximum-likelihood trees were generated using FastTree version 2.1.3 SSE3 using the Jones-Taylor-Thornton (JTT) model + CAT approximation with 20 rate categories. Branch support was calculated using the Shimodaira-Hasegawa (SH) test with 1,000 resamples. Trees were displayed using Fig Tree v1.4.3 (http://tree.bio.ed.ac.uk/software/figtree/).

Strains, media, and growth conditions. All *M. acetivorans* strains were grown in single-cell morphology (61) in bicarbonate-buffered high salt (HS) liquid medium containing 125 mM methanol, 50 mM trimethylamine hydrochloride (TMA), 40 mM sodium acetate, or 20 mM dimethylsufide (DMS). Cultures were grown in sealed tubes with N_2/CO_2 (80/20) at 8-10 psi in the headspace. Most substrates were added to the medium prior to autoclaving. DMS was added from an anaerobic stock solution maintained at 4 °C immediately prior to inoculation. Growth rate measurements were conducted with three independent biological replicate cultures acclimated to the energy substrate or temperature as indicated. A 1:10 dilution of a late-exponential phase culture was used as the inoculum for growth rate measurement. Plating on HS

297 medium containing 50 mM TMA solidified with 1.7 % agar was conducted in an anaerobic glove
298 chamber (Coy Laboratory Products, Grass Lake, MI) as described previously in (62). Solid
299 media plates were incubated in an intra-chamber anaerobic incubator maintained at 37 °C with
300 $N_2/CO_2/H_2S$ (79.9/20/0.1) in the headspace as described previously in (63). Puromycin
301 (CalBiochem, San Diego, CA) was added to a final concentration of 2 μg/mL from a sterile,
302 anaerobic stock solution to select for transformants containing the *pac* (puromycin
303 transacetylase) cassette. The purine analog 8-aza-2,6-diaminopurine (8ADP) (R. I. Chemicals,
304 Orange, CA) was added to a final concentration of 20 μg/mL from a sterile, anaerobic stock
305 solution to select against the *hpt* (phosphoribosyltransferase) cassette encoded on pC2A-based
306 plasmids. *E. coli* strains were grown in LB broth at 37 °C with standard antibiotic
307 concentrations. WM4489, a DH10B derivative engineered to control copy-number of oriV-based
308 plasmids (64), was used as the host strain for all plasmids generated in this study (Supplementary
309 File 1). Plasmid copy number was increased dramatically by supplementing the growth medium
310 with sterile rhamnose to a final concentration of 10 mM.

311 **Plasmids.** All plasmids used in this study are listed in Supplementary File 1. Plasmids for
312 Cas9-mediated genome editing were designed as described previously in (40). Standard
313 techniques were used for the isolation and manipulation of plasmid DNA. WM4489 was
314 transformed by electroporation at 1.8 kV using an *E. coli* Gene Pulser (Bio-Rad, Hercules, CA).

315 All pDN201-derived plasmids were verified by Sanger sequencing at the Roy J. Carver
316 Biotechnology Center, University of Illinois at Urbana-Champaign and all pAMG40 cointegrates
317 were verified by restriction endonuclease analysis.

318 ***In silico* design of sgRNAs for gene-editing.** All target sequences used for Cas9-
319 mediated genome editing in this study are listed in Supplementary File 2. Target sequences were
320 chosen using the CRISPR site finder tool in Geneious version R9 (60). The *M. acetivorans*
321 chromosome and the plasmid pC2A were used to score off-target binding sites.

322 **Transformation of *M. acetivorans*.** All *M. acetivorans* strains used in this study are
323 listed in Supplementary File 3. Liposome-mediated transformation was used for *M. acetivorans*
324 as described previously in (65) using 10 mL of late-exponential phase culture of *M. acetivorans*
325 and 2 μg of plasmid DNA for each transformation.

326 **In-gel tryptic digest of McrA.** Mid-exponential phase cultures of *M. acetivorans* grown
327 in 10 mL HS medium containing 50 mM TMA were harvested by centrifugation at 5,000 RPM
328 (3,000 × *g*) for 15 minutes in a Sorvall RC500 Plus centrifuge maintained at 4 °C (DuPont,
329 Wilmington, DE) using a SS-34 rotor. The cell pellet was resuspended in 1 mL lysis buffer (50
330 mM NH_4HCO_3, pH = 8.0) and harvested by centrifugation at 12,000 RPM (17,500 × *g*) for 30
331 minutes in a Sorvall RC500 Plus centrifuge maintained at 4 °C (DuPont, Wilmington, DE) using
332 a SS-34 rotor. An equal volume of the supernatant was mixed with 2x Laemmli sample buffer

(Bio-Rad, Hercules, CA) containing 5% β-mercaptoethanol, incubated in boiling water for 10 mins, loaded on a 4-20% gradient Mini-Protean TGX denaturing SDS-PAGE gel (Bio-Rad, Hercules, CA) and run at 70 V until the dye-front reached the bottom of the gel. The gel was stained using the Gel Code Blue stain reagent (Thermo Fisher Scientific, Waltham, MA) as per the manufacturer's instructions. Bands corresponding to McrA (*ca*. 60 kDa) were excised and cut into *ca*. 1 × 1 mm cubes. The gel slices from a single well were destained with 50% acetonitrile, the corresponding protein was reduced with 10 mM DTT, and digested with 1.5 μg sequencing-grade trypsin (Promega, Madison, WI) at 37 °C for 16-20 hours in the presence of 5% (*v*/*v*) *n*-propanol. The digested peptides were extracted and dried as described previously (66).

MS analysis of tryptic peptides. MALDI-TOF-MS analysis was performed using a Bruker UltrafleXtreme MALDI TOF-TOF mass spectrometer (Bruker Daltonics, Billerica, MA) in reflector positive mode at the University of Illinois School of Chemical Sciences Mass Spectrometry Laboratory. The samples were desalted using C-18 zip-tips using acetonitrile and water as solvent system and sinapic acid in 70% acetonitirile was used as the matrix. Data analysis was carried out using the Bruker FlexAnalysis software. For HR-ESI MS/MS, samples were dissolved in 35% aq. acetonitrile and 0.1% formic acid. Samples were directly infused using an Advion TriVersa Nanomate 100 into a ThermoFisher Scientific Orbitrap Fusion ESI-MS. The instrument was calibrated weekly, following the manufacturer's instructions, and tuned

daily with Pierce LTQ Velos ESI Positive Ion Calibration Solution (Thermo Fisher Scientific, Waltham, MA). The MS was operated using the following parameters: resolution, 100,000; isolation width (MS/MS), 1 *m/z*; normalized collision energy (MS/MS), 35; activation q value (MS/MS), 0.4; activation time (MS/MS), 30 ms. Data analysis was conducted using the Qualbrowser application of Xcalibur software (Thermo Fisher Scientific, Waltham, MA). HPLC-grade reagents were used to prepare samples for mass spectrometric analyses.

Funding Information

The authors acknowledge the Division of Chemical Sciences, Geosciences, and Biosciences, Office of Basic Energy Sciences of the U.S. Department of Energy through Grant DE-FG02-02ER15296 (to W.W.M) for the genetic and physiological studies in *Methanosarcina acetivorans*; the National Institutes of Health grant GM097142 (to D.A.M) for mass spectrometry experiments; and the Carl R. Woese Institute for Genomic Biology postdoctoral fellowship (to D.D.N). D.D.N is currently a Simons Foundation fellow of the Life Sciences Research Foundation. The funders had no role in study design, data collection and interpretation, or the decision to submit the work for publication.

Acknowledgements

We thank Graham A. Hudson (D.A.M. lab) for technical assistance with the HR and tandem MS data acquisition.

References

1. Ermler U, Grabarse W, Shima S, Goubeaud M, Thauer RK (1997) Crystal structure of Methyl-coenzyme M reductase : The key enzyme of biological methane formation. *Science* 278(5342):1457–1463.
2. Scheller S, Goenrich M, Boecher R, Thauer RK, Jaun B (2010) The key nickel enzyme of methanogenesis catalyses the anaerobic oxidation of methane. *Nature* 465(7298):606–608.
3. Wongnate T, Sliwa D, Ginovska B, Smith D, Wolf MW, Lehnert N, Raugei S, Ragsdale SW (2016) The radical mechanism of biological methane synthesis by methyl-coenzyme M reductase. *Science* 352(6288):953–958.
4. Thauer RK, Kaster A, Seedorf H, Buckel W, Hedderich R (2008) Methanogenic archaea: ecologically relevent differences in energy conservation. *Nature Rev Microbiol* 6(8):579–592.
5. Zheng K, Ngo PD, Owens VL, Yang X, Mansoorabadi SO (2016) The biosynthetic pathway of coenzyme F430 in methanogenic and methanotrophic archaea. *Science* 354(6310):339-342.
6. Moore SJ, Sowa ST, Schuchardt C, Deery E, Lawrence AD, Ramos JV, Billig S, Birkemeyer C, Chivers PT, Howard MJ, Rigby SEJ, Layer G, Warren MJ (2017) Elucidation of the biosynthesis of the methane catalyst coenzyme F430. *Nature* 543(7643):78–82.
7. Goubeaud M, Schreiner G, Thauer RK (1997) Purified methyl-coenzyme-M reductase is activated when the enzyme-bound coenzyme F430 is reduced to the nickel(I) oxidation state by titanium(III) citrate. *Eur J Biochem* 243:110–114.
8. Selmer T, Kahnt J, Goubeaud M, Shima S, Grabarse W, Ermler U, Thauer RK (2000) The biosynthesis of methylated amino acids in the active site region of methyl-coenzyme M reductase. *J Biol Chem* 275(6):3755–3760.
9. Kahnt J, Buchenau B, Mahlert F, Krüger M, Shima S, Thauer RK (2007) Post-translational modifications in the active site region of methyl-coenzyme M reductase from methanogenic and methanotrophic archaea. *FEBS J* 274(18):4913–4921.
10. Wagner T, Kahnt J, Ermler U, Shima S (2016) Didehydroaspartate modification in methyl-coenzyme M reductase catalyzing methane formation. *Angew Chemie - Int Ed* 55(36):10630–10633.
11. Grabarse W, Mahlert F, Shima S, Thauer RK, Ermler U (2000) Comparison of three methyl-coenzyme M reductases from phylogenetically distant organisms : unusual amino acid modification , conservation and adaptation. *J Mol Biol* 303(2):329-344
12. Grabarse W, Mahlert F, Duin EC, Goubeaud M, Shima S, Thauer RK, Lamzin V, Ermler

U (2001) On the mechanism of biological methane formation: structural evidence for conformational changes in methyl-coenzyme M reductase upon substrate binding. *J Mol Biol* 309(1):315–330.

13. Horng Y, Becker DF, Ragsdale SW (2001) Mechanistic studies of methane biogenesis by methyl-coenzyme M reductase: evidence that coenzyme B participates in cleaving the C - S Bond of methyl-coenzyme M. *Biochemistry* 40(43):12875–12885.
14. Pan M, Mabry TJ, Beale JM, Mamiya BM (1997) Nonprotein amino acids from *Cycas revoluta*. *Phytochemistry* 45(3):517–519.
15. Hayakawa Y, Sasaki K, Nagai K, Shin-ya K, Furihata K (2006) Structure of thioviridamide, a novel apoptosis inducer from Streptomyces *olivoviridis*. *J Antibiot* 59(1):6–10.
16. Kim HJ, Graham DW, DiSpirito AA, Alterman MA, Galeva N, Larive CK, Asunskis D, Sherwood PMA (2004) Methanobactin, a copper-acquisition compound from methane-oxidizing bacteria. *Science* 305(5690):1612–1615.
17. Kenney GE, Rosenzweig AC (2012) Chemistry and biology of the copper chelator methanobactin. *ACS Chem Biol* 7(2):260-268.
18. Kenney GE, Rosenzweig AC (2013) Genome mining for methanobactins. *BMC Biology* 11(1):17.
19. Lincke T, Behnken S, Ishida K, Roth M, Hertweck C (2013) Closthioamide : an unprecedented polythioamide antibiotic from the strictly anaerobic bacterium *Clostridium cellulolyticum*. *Angew Chemie Int Ed* 122(11):2055-2057.
20. Chiriac AI, Kloss F, Kramer J, Vuong C, Hertweck C, Sahl H-G (2015) Mode of action of closthioamide: the first member of the polythioamide class of bacterial DNA gyrase inhibitors. *J Antimicrob Chemother* 70:2576–2588.
21. Coyne S, Litomska A, Chizzali C, Khalil MNA, Richter K, Beerhues L, Hertweck C. (2014). Control of plant defense mechanisms and fire blight pathogenesis through the regulation of 6-thioguanine biosynthesis in *Erwinia amylovora*. *ChemBioChem* 15(3):373–376.
22. Puar MS, Ganguly AK, Afonso A, Brambilla R, Mangiaracina P (1981) Sch 18640. A new thiostrepton-type antibiotic. *J Am Chem Soc* 103(17):5231–5233.
23. Hensens OD, Albers-Schönberg G (1983) Total structure of the highly modified peptide antibiotic components of thiopeptin. *J Antibiot* 36(7):814–831.
24. Izawa M, Kawasaki T, Hayakawa Y (2013) Cloning and heterologous expression of the thioviridamide biosynthesis gene cluster from *Streptomyces olivoviridis*. *Appl Environ Microbiol* 79(22):7110–7113.
25. Dunbar KL, Melby JO, Mitchell DA (2012) YcaO domains use ATP to activate amide

backbones during peptide cyclodehydrations. *Nat Chem Biol* 8(6):569–575.

26. Dunbar KL, Chekan JR, Cox CL, Burkhart BJ, Nair SK, Mitchell DA (2014) Discovery of a new ATP-binding motif involved in peptidic azoline biosynthesis. *Nat Chem Biol* 10(10)823-829.

27. Arnison PG, Bibb MJ, Bierbaum G, Bowers A a, Bugni TS, Bulaj G, Camarero JA, Campopiano DJ, Challis GL, Clardy J, Cotter PD, Craik DJ, Dawson M, Dittmann E, Donadio S, Dorrestein PC, Entian K-D, Fischbach M a, Garavelli JS, Göransson U, Gruber CW, Haft DH, Hemscheidt TK, Hertweck C, Hill C, Horswill AR, Jaspars M, Kelly WL, Klinman JP, Kuipers OP, Link a J, Liu W, Marahiel M a, Mitchell D a, Moll GN, Moore BS, Müller R, Nair SK, Nes IF, Norris GE, Olivera BM, Onaka H, Patchett ML, Piel J, Reaney MJT, Rebuffat S, Ross RP, Sahl H-G, Schmidt EW, Selsted ME, Severinov K, Shen B, Sivonen K, Smith L, Stein T, Süssmuth RD, Tagg JR, Tang G-L, Truman AW, Vederas JC, Walsh CT, Walton JD, Wenzel SC, Willey JM, van der Donk WA (2013) Ribosomally synthesized and post-translationally modified peptide natural products: overview and recommendations for a universal nomenclature. *Nat Prod Rep* 30(1):108–160.

28. Burkhart BJ, Schwalen CJ, Mann G, Naismith JH, Mitchell DA. 2017. YcaO-dependent posttranslational amide activation: biosynthesis, structure, and function. *Chem Rev* DOI: 10.1021/acs.chemrev.6b00623.

29. Burkhart BJ, Hudson GA, Dunbar KL, Mitchell DA (2015) A prevalent peptide-binding domain guides ribosomal natural product biosynthesis. *Nat Chem Biol* 11(8):564–570.

30. Dunbar KL, Tietz JI, Cox CL, Burkhart BJ, Mitchell DA (2015) Identification of an auxiliary leader peptide-binding protein required for azoline formation in ribosomal natural products. *J Am Chem Soc* 137(24):7672–7677.

31. Wright CM, Christman GD, Snellinger AM, Johnston M V, Mueller EG (2006) Direct evidence for enzyme persulfide and disulfide intermediates during 4-thiouridine biosynthesis. *Chem Commun* 29:3104–3106.

32. Coyne S, Chizzali C, Khalil MNA, Litomska A, Richter K, Beerhues L, Hertweck C (2013) Biosynthesis of the antimetabolite 6-thioguanine in *Erwinia amylovora* plays a key role in fire blight pathogenesis. *Angew Chemie - Int Ed* 125(40):10564–10568.

33. Palenchar PM, Buck CJ, Cheng H, Larson TJ, Mueller EG (2000) Evidence that ThiI, an enzyme shared between thiamin and 4-thiouridine biosynthesis, may be a sulfurtransferase that proceeds through a persulfide intermediate. *J Biol Chem* 275(12):8283–8286.

34. Basu MK, Selengut JD, Haft DH (2011) ProPhylo : partial phylogenetic profiling to guide protein family construction and assignment of biological process. *BMC Bioinformatics* 12(1):434.

35. Borrel G, O'Toole PW, Harris HMB, Peyret P, Brugère JF, Gribaldo S Borrel G. (2013) Phylogenomic data support a seventh order of methylotrophic methanogens and provide insights into the evolution of methanogenesis. *Genome Biol Evol* 5(10):1769–1780.
36. Vanwonterghem I, Evans PN, Parks DH, Jensen PD, Woodcroft BJ, Hugenholtz P, Tyson GW (2016) Methylotrophic methanogenesis discovered in the archaeal phylum Verstraetearchaeota. *Nat Microbiol* 1:16170.
37. Zhang W, Urban A, Mihara H, Leimkühler S, Kurihara T, Esaki N. (2010) IscS functions as a primary sulfur-donating enzyme by interacting specifically with *moeB* and *moaD* in the biosynthesis of molybdopterin in *Escherichia coli*. *J Biol Chem* 285(4):2302–2308.
38. Park JH, Dorrestein PC, Zhai H, Kinsland C, McLafferty FW, Begley TP (2003) Biosynthesis of the thiazole moiety of thiamin pyrophosphate (vitamin B1). *Biochemistry* 42 (42):12430–12438.
39. Guss AM, Rother M, Zhang JK, Kulkarni G, Metcalf WW (2008) New methods for tightly regulated gene expression and highly efficient chromosomal integration of cloned genes for *Methanosarcina* species. *Archaea* 2(3):193–203.
40. Nayak DD, Metcalf WW (2017) Cas9-mediated genome editing in the methanogenic archaeon *Methanosarcina acetivorans*. *Proc Natl Acad Sci* DOI: 10.1073/pnas.1618596114
41. Wiberg KB, Rablen PR (1995) Why does thioformamide have a larger rotational barrier than formamide? *J Am Chem Soc* 117(8):2201–2209.
42. Perler FB, Xu MQ, Paulus H (1997) Protein splicing and autoproteolysis mechanisms. *Curr Opin Chem Biol* 1(3):292–299.
43. Schulman BA, Wade Harper J (2009) Ubiquitin-like protein activation by E1 enzymes: the apex for downstream signalling pathways. *Nat Rev Mol Cell Biol* 10(5):319–331.
44. Matthies A, Nimtz M, Leimkühler S (2005) Molybdenum cofactor biosynthesis in humans: Identification of a persulfide group in the rhodanese-like domain of MOCS3 by mass spectrometry. *Biochemistry* 44(21):7912–7920.
45. Galagan JE, Nusbaum C, Roy A, Endrizzi MG, Macdonald P, Fitzhugh W, Calvo S, Engels R, Smirnov S, Atnoor D, Brown A, Allen N, Naylor J, Stange-thomann N, Dearellano K, Johnson R, Linton L, Mcewan P, Mckernan K, Talamas J, Tirrell A, Ye W, Zimmer A, Barber RD, Cann I, Graham DE, Grahame DA, Guss AM, Hedderich R, Ingram-smith C, Kuettner HC, Krzycki JA, Leigh JA, Li W, Liu J, Mukhopadhyay B, Reeve JN, Smith K, Springer TA, Umayam LA, White O, White RH, Macario EC De, Ferry JG, Jarrell KF, Jing H, Macario AJL, Paulsen I, Pritchett M, Sowers KR, Swanson R V, Zinder SH, Lander E, Metcalf WW, Birren B (2002) The Genome of *M. acetivorans* reveals extensive metabolic and physiological diversity. *Genome Research* 12(4):532–

542.

46. Deppenmeier U, Lienard T, Gottschalk G (1999) Novel reactions involved in energy conservation by methanogenic archaea. *FEBS Lett* 457(3):291-297.

47. Bose A, Pritchett MA, Metcalf WW (2008) Genetic analysis of the methanol- and methylamine-specific methyltransferase 2 genes of *Methanosarcina acetivorans* C2A. *J Bacteriol* 190(11):4017–4026.

48. Fu H, Metcalf WW (2015) Genetic basis for metabolism of methylated sulfur compounds in *Methanosarcina* species. *J Bacteriol* 197(8):1515–1524.

49. Schönheit P, Kristjansson JK, Thauer RK (1982) Kinetic mechanism for the ability of sulfate reducers to out-compete methanogens for acetate. *Arch Microbiol* 132(3):285–288.

50. Finster K, Tanimoto T, Bak F (1992) Fermentation of methanethiol and dimethylsulfide by a newly isolated methanogenic bacterium. *Arch Microbiol* 152(5):425–430.

51. Patterson JA, Hespell RB (1979) Trimethylamine and methylamine as growth substrates for rumen bacteria and *Methanosarcina barkeri*. *Curr Microbiol* 3(2):79–83.

52. Rospert S, Linder D, Ellerman J, Thauer RK (1990) Two genetically distinct methyl-coenzyme M reductases in *Methanobacterium thermoautotrophicum* strain Marburg and ΔH. *Eur J Biochem* 194(3):871–877.

53. Petersson EJ, Goldberg JM, Wissner RF (2014) On the use of thioamides as fluorescence quenching probes for tracking protein folding and stability. *Phys Chem Chem Phys* 16(15):6827–6837.

54. Lee HJ, Choi YS, Lee KB, Park J, Yoon CJ (2002) Hydrogen bonding abilities of thioamide. *J Phys Chem A* 106(30):7010–7017.

55. Gribaldo S, Brochier-Armanet C (2006) The origin and evolution of Archaea: a state of the art. *Philos Trans R Soc B* 361(1470):1007–1022.

56. Forterre P (2015) The universal tree of life: an update. *Front Microbiol* 6:1–18.

57. Weiss MC, Sousa FL, Mrnjavac N, Neukirchen S, Roettger M, Nelson-Sathi S, Martin WF(2016) The physiology and habitat of the last universal common ancestor. *Nat Microbiol* 1:16116.

58. Franzmann PD, Springer N, Ludwig W, Conway De Macario E, Rohde M (1992) A methanogenic archaeon from Ace Lake, Antarctica: *Methanococcoides burtonii* sp. nov. *Syst Appl Microbiol* 15(4):573–581.

59. Edgar RC (2004) MUSCLE: Multiple sequence alignment with high accuracy and high throughput. *Nucleic Acids Res* 32(5):1792–1797.

60. Kearse M, Moir R, Wilson A, Stones-Havas S, Cheung M, Sturrock S, Buxton S, Cooper A, Markowitz S, Duran C, Thierer T, Ashton B, Meintjes P, Drummond A. (2012) Geneious Basic: An integrated and extendable desktop software platform for the

548 organization and analysis of sequence data. *Bioinformatics* 28(12):1647–1649.
549 61. Sowers KR, Boone JE, Gunsalus RP (1993) Disaggregation of *Methanosarcina* spp. and
550 growth as single cells at elevated osmolarity. *Appl Environ Microbiol* 59(11):3832–3839.
551 62. Metcalf WW, Zhang JK, Shi X, Wolfe RS (1996) Molecular, genetic, and biochemical
552 characterization of the *serC* gene of *Methanosarcina barkeri* Fusaro. *J Bacteriol*
553 178(19):5797–5802.
554 63. Metcalf WW, Zhang JK, Wolfe RS (1998) An anaerobic, intrachamber incubator for
555 growth of *Methanosarcina* spp. on methanol-containing solid media. *Appl Environ*
556 *Microbiol* 64(2):768–770.
557 64. Kim SY, Ju KS, Metcalf WW, Evans BS, Kuzuyama T, Van Der Donk WA. (2012)
558 Different biosynthetic pathways to fosfomycin in *Pseudomonas syringae* and
559 *Streptomyces* species. *Antimicrob Agents Chemother* 56(8):4175–4183.
560 65. Metcalf WW, Zhang J, Apolinario E, Sowers KR, Wolfe RS (1997) A genetic system for
561 Archaea of the genus *Methanosarcina*: Liposome-mediated transformation and
562 construction of shuttle vectors. *Proc Natl Acad. Sci* 94(6):2626–2631.
563 66. Shevchenko A, Tomas H, Havlis J, Olsen JV, Mann M (2006) In-gel digestion for mass
564 spectrometric characterization of proteins and proteomes. *Nat Protoc* 1(6):2856–2860.
565

Figure Legends

Figure 1. Comparison of reactions catalyzed by YcaO proteins. *Top*, Biochemically characterized YcaO proteins involved in the synthesis of azol(in)e-containing ribosomal natural products catalyze the ATP-dependent cyclodehydration of cysteine, serine, and threonine residues. Shown is the conversion of peptidic cysteine to thiazoline. This reaction proceeds via an *O*-phosphorylated hemiorthoamide intermediate. *Bottom*, An analogous reaction is believed to occur in the biosynthesis of the thioamide bond in thioviridamide. Rather than an adjacent cysteine acting as the nucleophile, an exogenous source of sulfide (S^{2-}) is required for this reaction. TfuA may mediate the delivery of sulfide equivalents for this reaction.

Figure 2. A maximum-likelihood phylogenetic tree of YcaO homologs in archaea. Taxa in green, blue, and orange depict methanogens and anaerobic methane oxidizing archaea (ANMEs) with sequenced genomes. Taxa shown in green contain a single copy of *ycaO* and *tfuA*, those in blue contain two copies of *ycaO* and one copy of *tfuA*, while those in orange contain one copy of *ycaO,* but do not encode *tfuA*. Taxa shown in pink are other archaea that also encode *ycaO* and *tfuA* homologs. The gene neighborhoods of selected taxa are also depicted, showing the common co-localization with genes annotated as having a role in sulfur metabolism or methanogenesis. The node labels indicate support values calculated using the Shiomdaira-Hasegawa test using

583 1000 resamples. Support values less than 0.5 have not been shown. The outgroup denotes a
584 variety of bacterial taxa.

585 **Figure 3. Panel A,** Experimental strategy for deletion of the *ycaO-tfuA* locus in *M. acetivorans*
586 using a Cas9-mediated genome editing technique. Co-expression the Cas9 protein along with a
587 single guide RNA (sgRNAs) with a 20 bp target sequence flanked by a 3' NGG protospacer
588 adjacent motif on the chromosome (PAM; in red) generates double-stranded breaks (DSBs) at
589 the *ycaO-tfuA* locus. Repair of this break via homologous recombination with an appropriate
590 repair template (HR Template) generates an in-frame deletion on the host chromosome. **Panel B,**
591 A Cas9-based assay for gene essentiality. Mean transformation efficiencies of plasmids with
592 (dark gray) or without (light gray) an appropriate repair template are shown. The known essential
593 gene *mcrA* is included as a positive control. The error bars represent one standard deviation of
594 three independent transformations.

595 **Figure 4. MALDI-TOF MS analysis of McrA**. *Top,* Spectrum obtained from WT tryptic
596 digests containing the thioglycine modified L461-R491 peptide (*m/z* 3432 Da). A small amount
597 of the unmodified L_{461}-R_{491} peptide (*m/z* 3416 Da) is also observed, which probably arises via
598 non-enzymatic hydrolysis of the thioamide bond as previously reported (9). *Bottom,* Spectrum
599 obtained from Δ*ycaO-tfuA* tryptic digests containing only the unmodified L461-R491 peptide

600 (*m/z* 3416 Da). The *m/z* 3375 Da species present in both samples corresponds to MCRα residues

601 D392-R421.

602 **Figure 5.** Growth rate of the WWM60 (WT; blue) and the Δ*ycaO-tfuA* mutant (green) in HS

603 medium with 125 mM methanol at the indicated temperatures. A statistically significant

604 difference ($p < 0.01$) using a two-tailed unpaired t-test is indicated with an *.

605 **Tables**

606 **Table 1**: Growth phenotypes of WWM60 (WT) and WWM992 (Δ*ycaO-tfuA*) on different

607 substrates at 36 ºC.

Substrate[a]	Strain	Doubling Time (h)[b]	p-value	Maximum OD_{600}[b]	p-value
Methanol	WT	6.94 ± 0.41	0.87	5.35 ± 0.31	0.26
	Δ*ycaO-tfuA*	6.89 ± 0.15		5.06 ± 0.39	
TMA	WT	10.92 ± 0.54	0.84	9.57 ± 0.67	0.31
	Δ*ycaO-tfuA*	10.98 ± 0.43		8.91 ± 0.73	
Acetate	WT	54.23 ± 4.03	**0.0002**	0.44 ± 0.01	**0.0005**
	Δ*ycaO-tfuA*	124.33 ± 12.52		0.35 ± 0.02	
DMS	WT	31.27 ± 1.28	**<0.0001**	0.60 ± 0.01	**<0.0001**
	Δ*ycaO-tfuA*	58.28 ± 1.45		0.44 ± 0.01	

608 [a]TMA, trimethyamine; DMS, dimethylsulfide.

609 [b]The error represents the 95% confidence interval of the mean for three biological replicates and

610 the p-values were calculated using two-tailed unpaired t-tests.

611

612 **Supplementary Files**

613 **Supplementary File 1**– Lists of plasmids

614 **Supplementary File 2** – List of target sequences for Cas9-mediated genome editing

615 **Supplementary File 3** – List of strains

616

617 **Legends for Figure Supplements**

618 **Figure 2 – Supplementary Figure 1. Panel A)** Unrooted maximum-likelihood phylogeny of
619 1,000 YcaO sequences retrieved from the NCBI non-redundant protein sequence database using
620 the corresponding sequence from *Methanosarcina acetivorans* as a search query. **Panel B)**
621 Unrooted maximum-likelihood phylogeny of 1, 000 TfuA sequences retrieved from the NCBI
622 non-redundant protein sequence database using the corresponding sequence from *M. acetivorans*
623 as a search query. Divergent archaea-derived sequences in the TfuA tree are denoted with an *.
624
625 **Figure 2 – Supplementary Figure 2.** Unrooted maximum-likelihood phylogeny of 1,000 TfuA
626 sequences retrieved from the NCBI non-redundant protein sequence database using the
627 corresponding sequence from *Methanosarcina acetivorans* as a search query. For taxa where
628 *tfuA* and *ycaO* are not adjacently encoded genes a gene architecture diagram is shown. The node
629 labels indicate support values calculated using the Shiomdaira-Hasegawa test using 1000
630 resamples. Support values less than 0.5 have not been shown. The outgroup is comprised of
631 various bacterial TfuA protein sequences.
632
633 **Figure 3 – Supplementary Figure 1.** A PCR-based screen to genotype the *ycaO-tfuA* locus in
634 *Methanosarcina acetivorans*. The PCR amplicon from three independently derived mutants
635 containing an unmarked in-frame deletion of *ycaO-tfuA* (Lanes 2-4) is 2980 bp whereas the
636 corresponding amplicon from a strain containing the wild-type locus is 4742 bp (Lane 5). Lanes
637 1 and 6 contain a 1 kb DNA ladder.
638

Figure 4 – Supplementary Figure 1. Panel A) High-resolutions electrospray ionization tandem mass spectrometry (HR-ESI MS/MS) analysis of a wild-type tryptic peptide from *Methanosarcina acetivorans* McrA (L_{461}-R_{491}, *m/z* 3432 Da). The b_6 ion localizes the thioamide modification to Gly_{465}. No b_5 ion was detected suggesting negligible fragmentation at the thioamide bond. Predicted masses and associated errors are shown. **Panel B)** HR-ESI-MS/MS analysis of the corresponding McrA tryptic peptide from the Δ*ycaO-tfuA* deletion strain of *M. acetivorans* (*m/z* 3416 Da). The b_5 and b_6 ion localizes the amide functionality at Gly_{465}. Predicted masses and associated errors are shown.

Figure 4 – Supplementary Figure 2. HR-ESI-MS/MS of the tryptic peptide from *Methanosarcina acetivorans* McrA (D_{392}-R_{421}, *m/z* 3375 Da) present in both the wild-type and Δ*ycaO-tfuA* deletion strain. Predicted masses and associated errors are shown.

Figure 4 – Supplementary Figure 3. Panel A) Matrix-assisted laser desorption/ionization time-of-flight mass spectrometry (MALDI-TOF MS) analysis of the wild-type (WT, top) and Δ*ycaO-tfuA* deletion strain (bottom) spectra identify the McrA tryptic peptide, H_{271}-R_{284} (*m/z* 1496 Da), containing the known *N*-methylhistidine modification. This suggests that the thioglycine formation is not a prerequisite for this methylation event. **Panel B)** MALDI-TOF MS analysis of the WT (top) and Δ*ycaO-tfuA* deletion strain (bottom) spectra identify the McrA tryptic peptide, F_{408}-R_{421}, (*m/z* 1561 Da). This peptide has been reported to contain a β-methylation at Q420 in other methanogens (9), however, it remains unmodified in *M. acetivorans*.

Figure 5 – Supplementary Figure 1. An overview of methanogenic metabolism in *M. acetivorans*. Methylotrophic substrates such as methanol (CH_3OH) or dimethylsulfide (DMS)

663 enter the methanogenic pathway via *S*-methylation of coenzyme M (CoM) and subsequent
664 disproportionation to methane (CH_4) and carbon dioxide (CO_2; metabolic flux is shown as blue
665 arrows). Notably, the first step in oxidation of CH_3-CoM to CO_2 is the energy-requiring transfer
666 of the methyl moiety to generate methyl-tetrahydrosarcinapterin (CH_3-H_4SPt). In contrast, acetic
667 acid enters the pathway at the CH_3-H_4SPt level, followed by reduction to CH_4 (green arrows).
668 Thus, the second step of the pathway is exergonic.

Figure 1

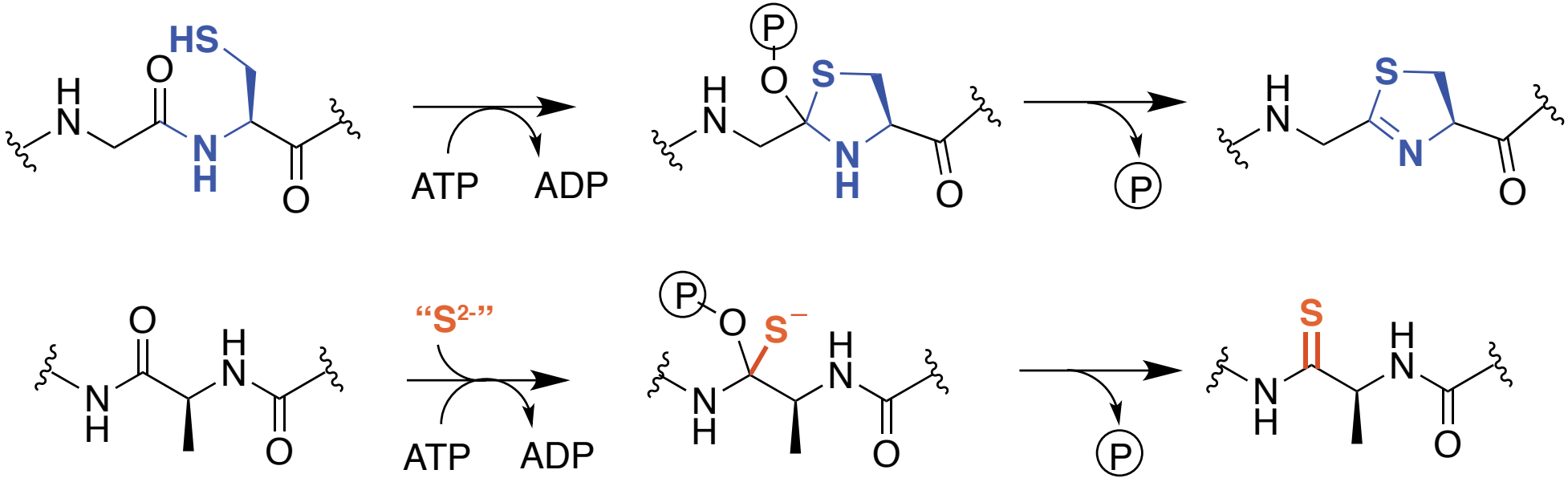

Fig. 1: Comparison of reactions catalyzed by YcaO proteins. **Top,** Biochemically characterized YcaO proteins involved in the synthesis of thiazole/oxazole modified microcin natural products catalyze the ATP-dependent cyclodehydration of peptidic cysteines to thiazolines. This reaction proceeds via an O-phosphorylated hemiorthoamide intermediate. **Bottom,** An analogous reaction is believed to occur in the synthesis of thioviridamide. Rather than an adjacent cysteine providing the nucleophile, an exogenous source of sulfide (S^{2-}), which may be delivered by TfuA, is required.

Figure 2

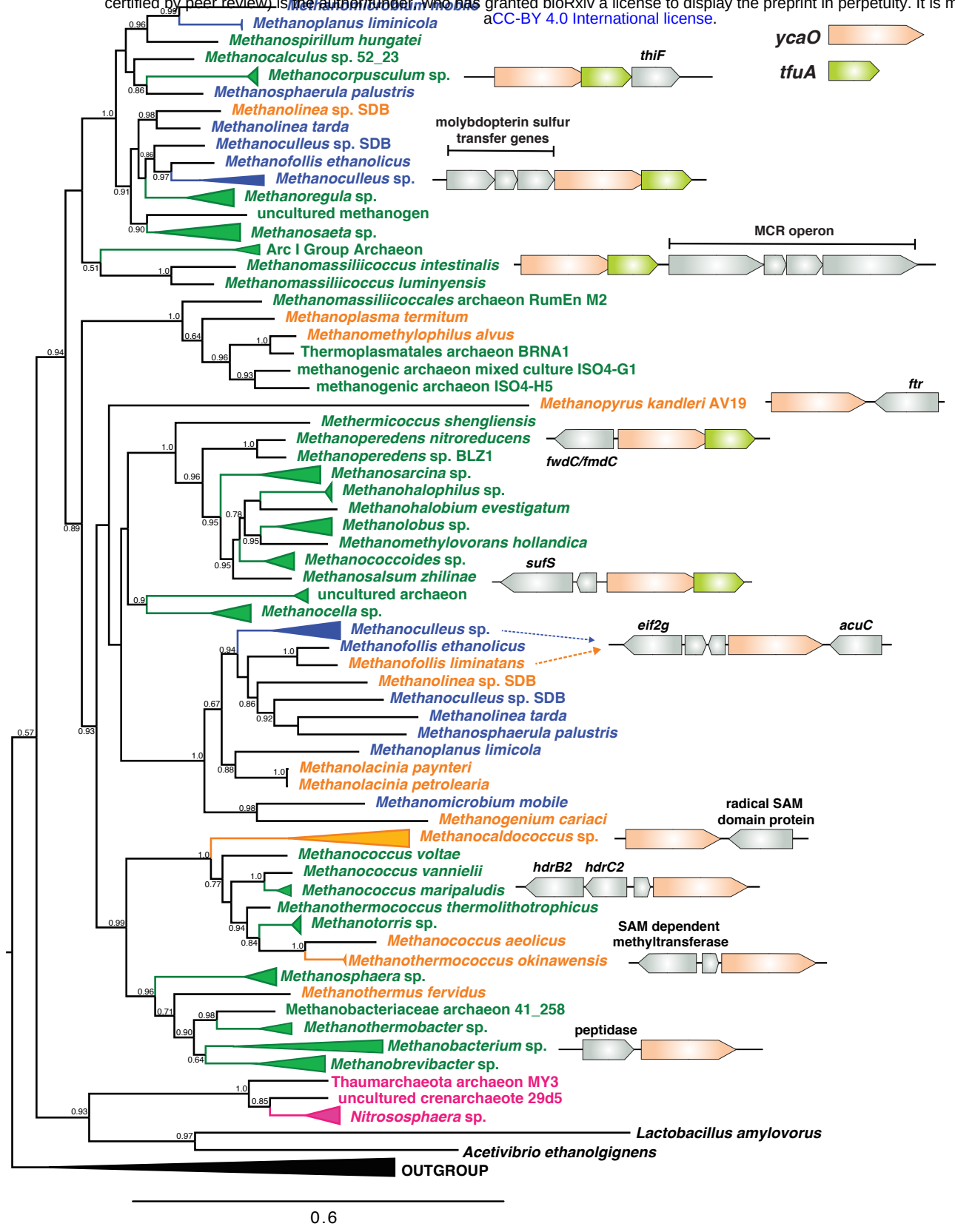

Fig. 2: A maximum-likelihood phylogenetic tree of YcaO homologs in archaea. Taxa in green, blue, and orange depict methanogens and anaerobic methane oxidizing archaea (ANMEs) with completely sequenced genomes. Taxa shown in green contain a single copy of *ycaO* and *tfuA*, those in blue contain two copies of *ycaO* and one copy of *tfuA*, while those in orange contain one copy of *ycaO*, but do not encode *tfuA*. Taxa shown in pink are other archaea that also encode *ycaO* and *tfuA* homologs. The gene neighborhoods of selected taxa are also depicted, showing the common co-localization with genes annotated as having a role in sulfur metabolism or methanogenesis. The node labels indicate support values calculated using the Shiomdaira-Hasegawa test using 1000 resamples. Support values less than 0.5 have not been shown. The outgroup denotes a variety of bacterial taxa.

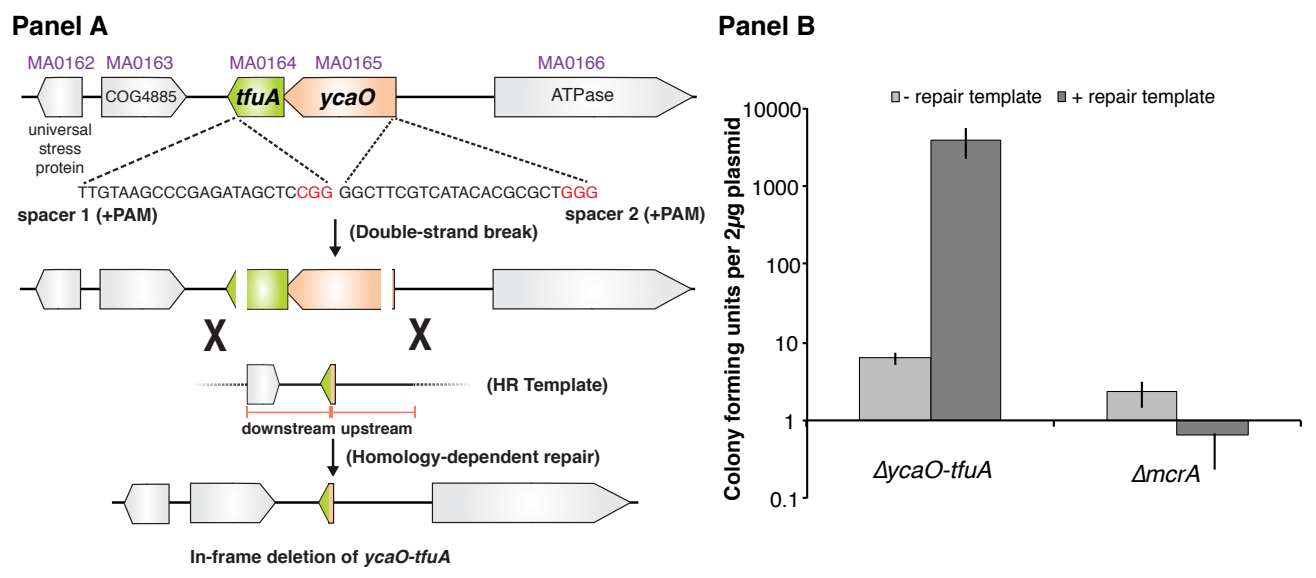

Fig. 3: Panel A, Experimental strategy for deletion of the *ycaO-tfuA* locus in *M. acetivorans* using a Cas9-mediated genome editing technique. Co-expression the Cas9 protein along with a single guide RNA (sgRNAs) with a 20 bp target sequence flanked by a 3' NGG protospacer adjacent motif on the chromosome (PAM; in red) generates double-stranded breaks (DSBs) at the *ycaO-tfuA* locus. Repair of this break via homologous recombination with an appropriate repair template (HR Template) generates an in-frame deletion on the host chromosome. **Panel B,** A Cas9-based assay for gene essentiality. Mean transformation efficiencies of plasmids with (dark gray) or without (light gray) an appropriate repair template are shown. The known essential gene *mcrA* is included as a positive control. The error bars represent one standard deviation of three independent transformations.

Figure 4

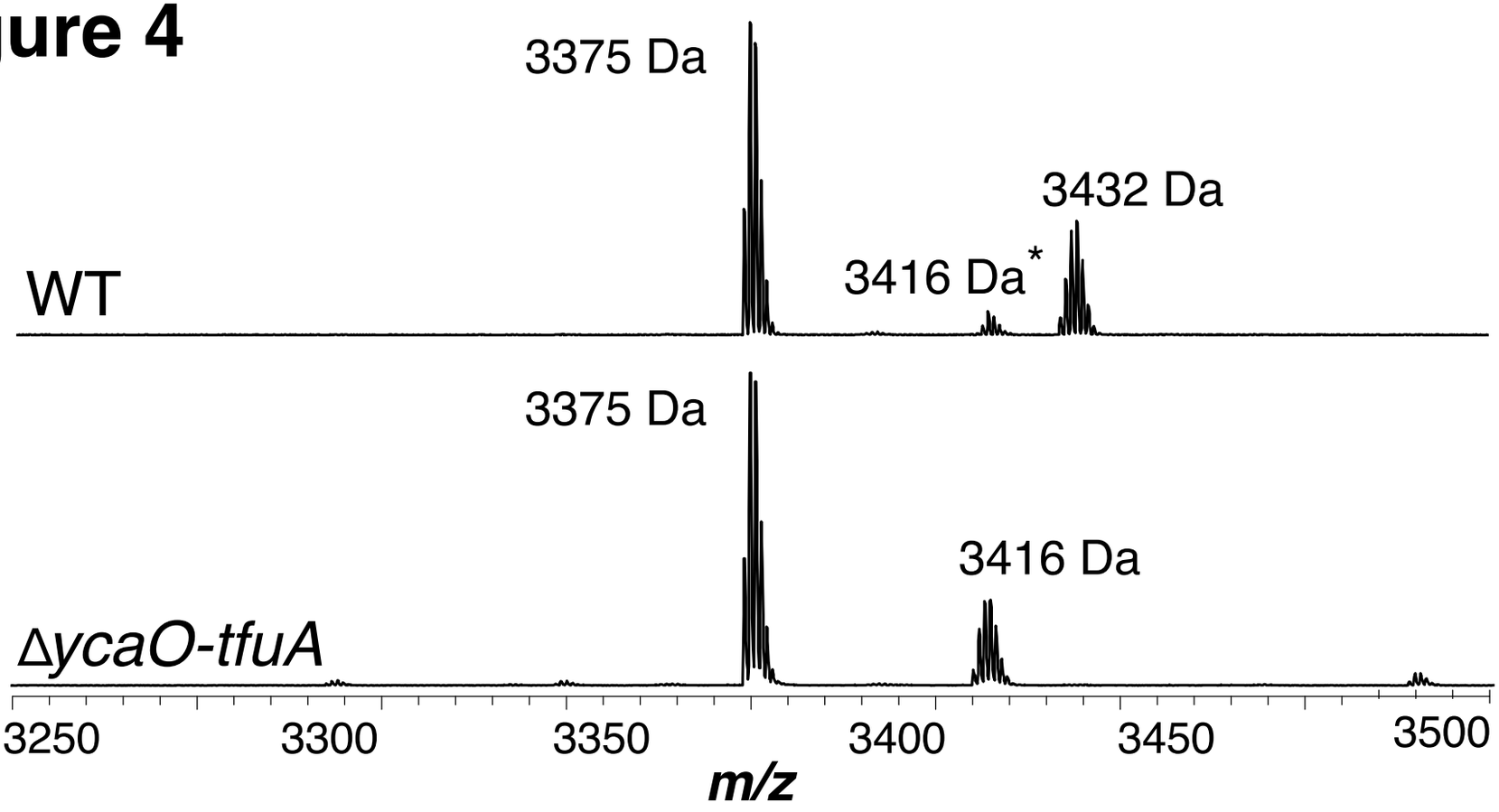

Fig. 4: MALDI-TOF MS analysis of MCRα. **Top,** Spectrum obtained from WT tryptic digests containing the thioglycine modified L461-R491 peptide (*m/z* 3432 Da). A small amount of the unmodified L461-R491 peptide (*m/z* 3416 Da) is also observed, which probably arises via non-enzymatic hydrolysis of the thioamide bond as previously reported (9). Bottom, Spectrum obtained from *Δ ycaO-tfuA* tryptic digests containing only the unmodified L461-R491 peptide (m/z 3416 Da). The m/z 3375 Da species present in both samples corresponds to MCRα residues D392-R421.

Figure 5

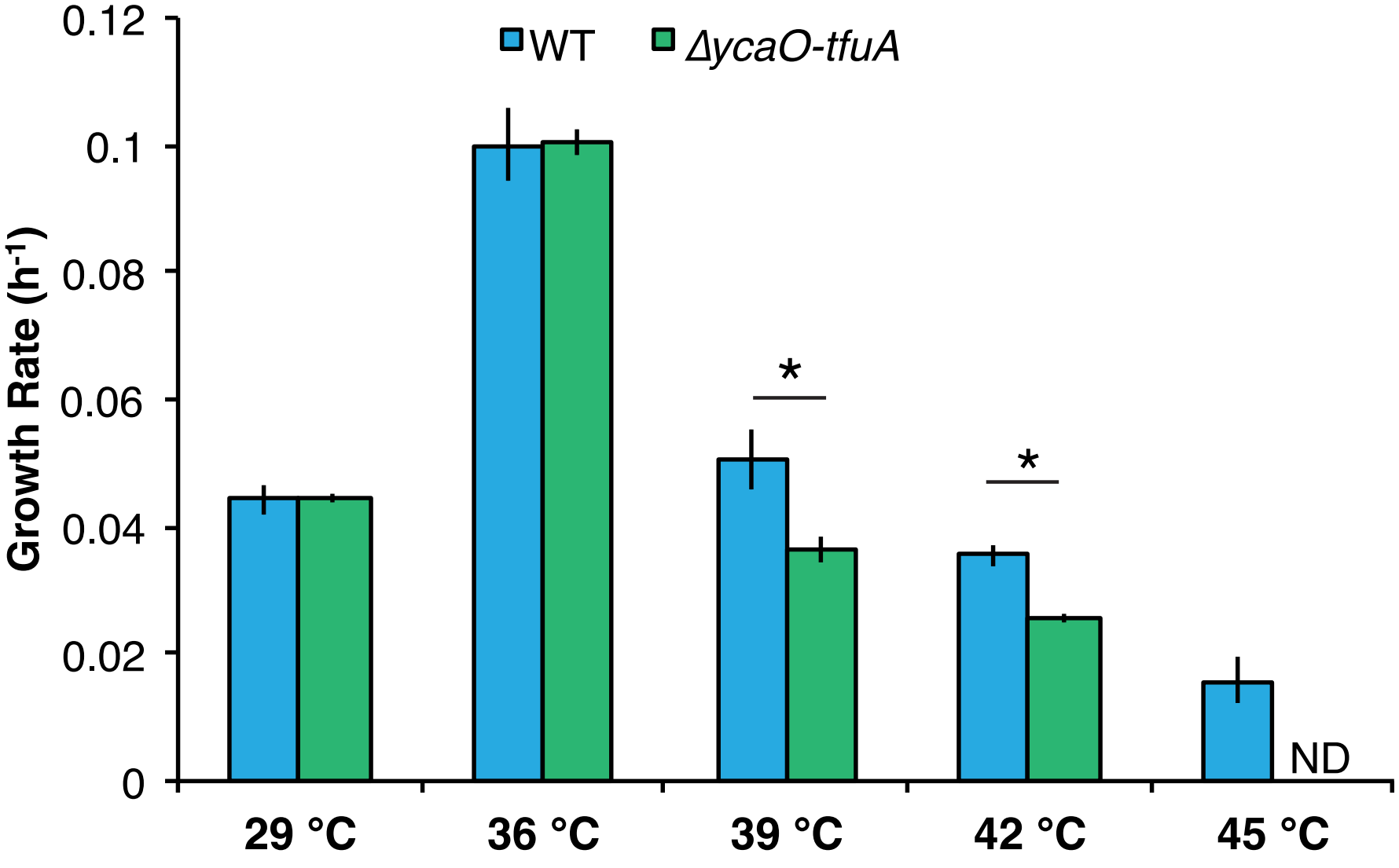

Fig. 5: Growth rate of the WWM60 (WT; blue) and the *ΔycaO-tfuA* mutant (green) in HS medium with 125 mM methanol at the indicated temperatures. A statistically significant difference ($p < 0.01$) using a two-tailed unpaired t-test is indicated with an *.
ND indicates that no growth was detected after one month of incubation.

Figure 2 - Supplementary Figure 1

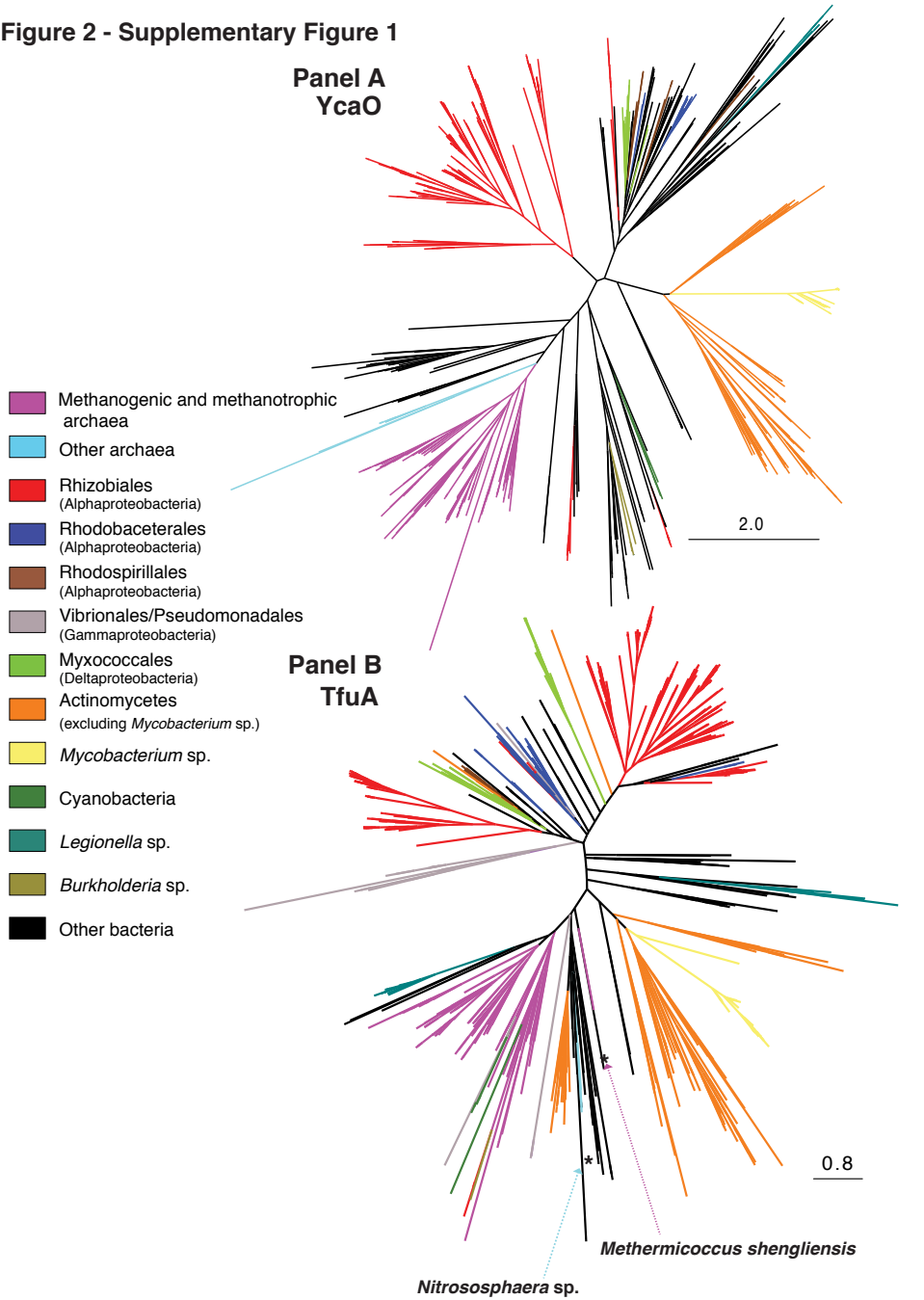

Fig. 2 - Supp Fig. 1: Panel A, Unrooted maximum-likelihood phylogeny of 1,000 YcaO sequences retrieved from the NCBI non-redundant protein sequence database using the corresponding sequence from *Methanosarcina acetivorans* as a search query. **Panel B,** Unrooted maximum-likelihood phylogeny of 1000 TfuA sequences retrieved from the NCBI non-redundant protein sequence database using the corresponding sequence from *M. acetivorans* as a search query. Divergent archaea-derived sequences on the TfuA tree are denoted with

Figure 2 - Supplementary Figure 2

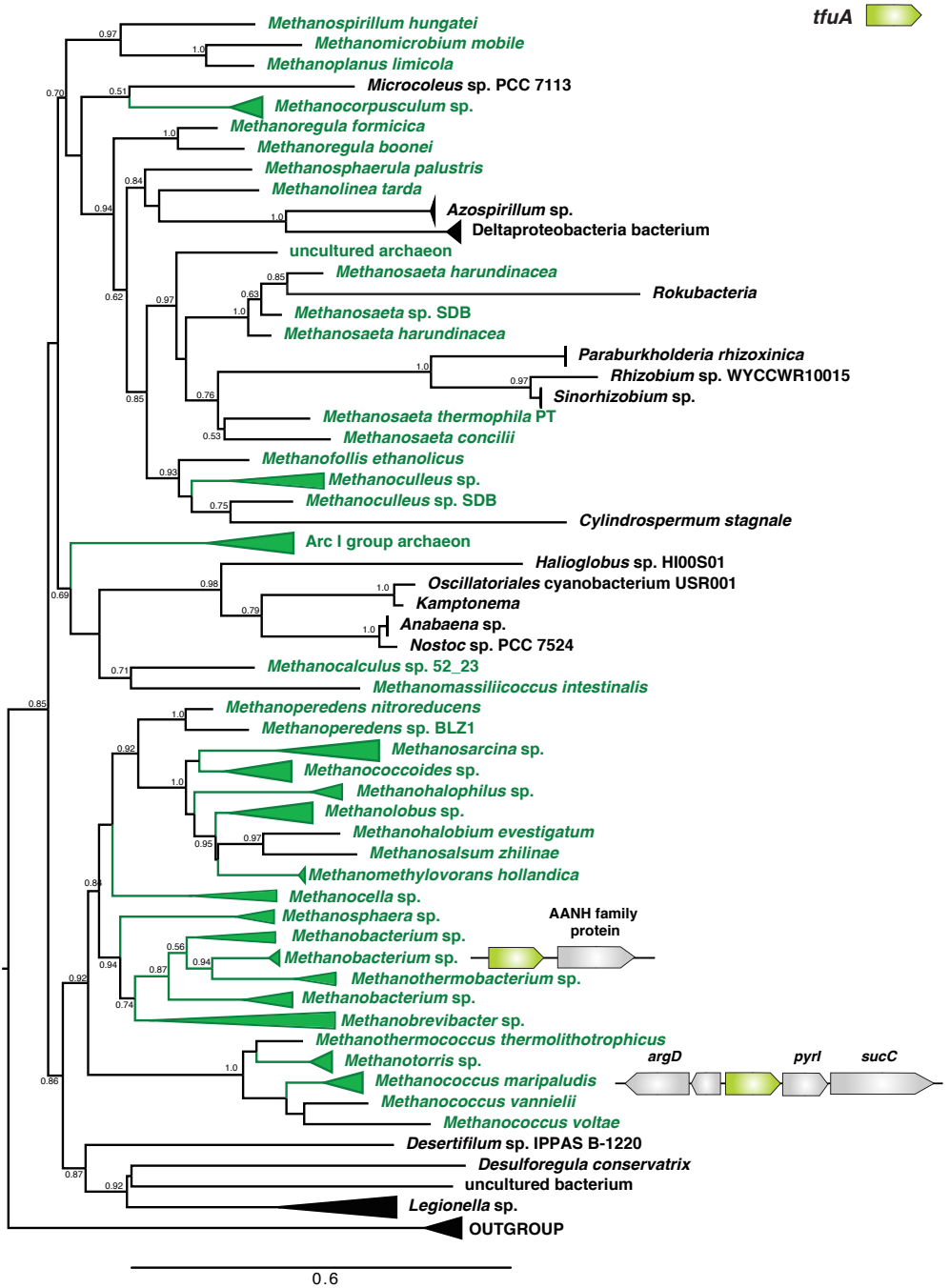

Fig. 2 - Supp. Fig. 2: Unrooted maximum-likelihood phylogeny of 1,000 TfuA sequences retrieved from the NCBI non-redundant protein sequence database using the corresponding sequence from *Methanosarcina acetivorans* as a search query. For taxa where *tfuA* and *ycaO* are not adjacently encoded genes a gene architecture diagram is shown. The node labels indicate support values calculated using the Shiomdaira-Hasegawa test using 1000 resamples. Support values less than 0.5 have not been shown. The outgroup is comprised of various bacterial TfuA protein sequences.

Figure 3 - Supplementary Figure 1

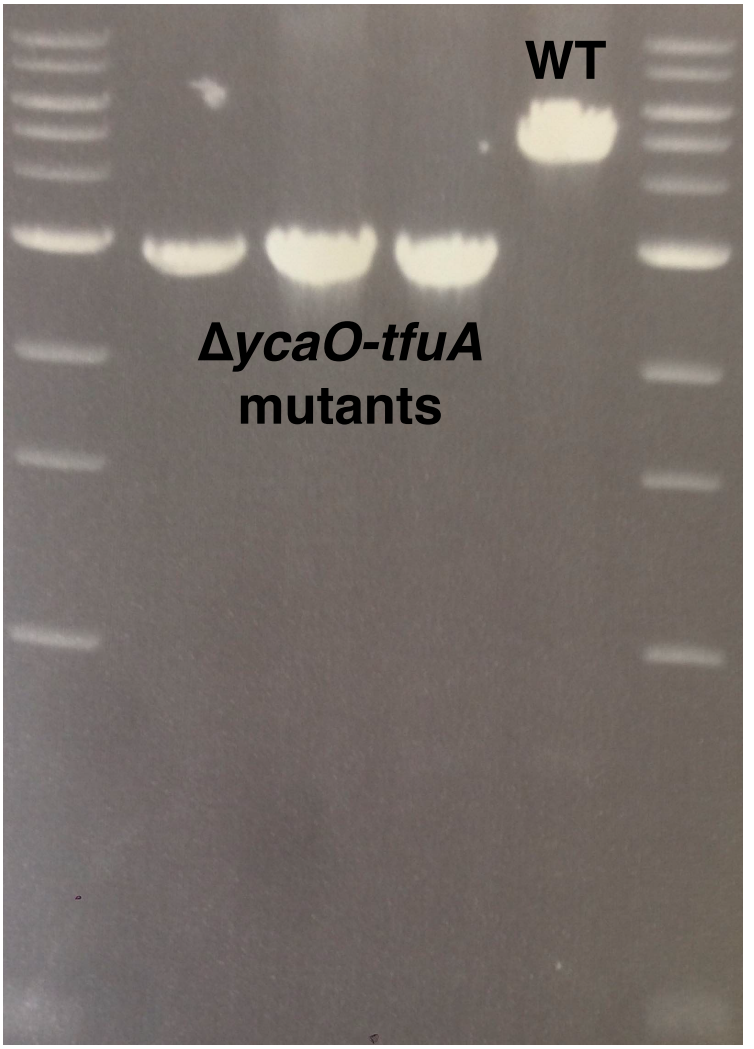

Fig. 3 - Supp. Fig. 1: A PCR-based screen to genotype the *ycaO-tfuA* locus in *Methanosarcina acetivorans*. The PCR amplicon from three independently derived mutants containing an unmarked in-frame deletion of *ycaO-tfuA* (Lanes 2-4) is 2980 bp whereas the corresponding amplicon from a strain containing the wild-type locus is 4742 bp (Lane 5). Lanes 1 and 6 contain a 1 kb DNA ladder.

Figure 4 - Supplementary Figure 1

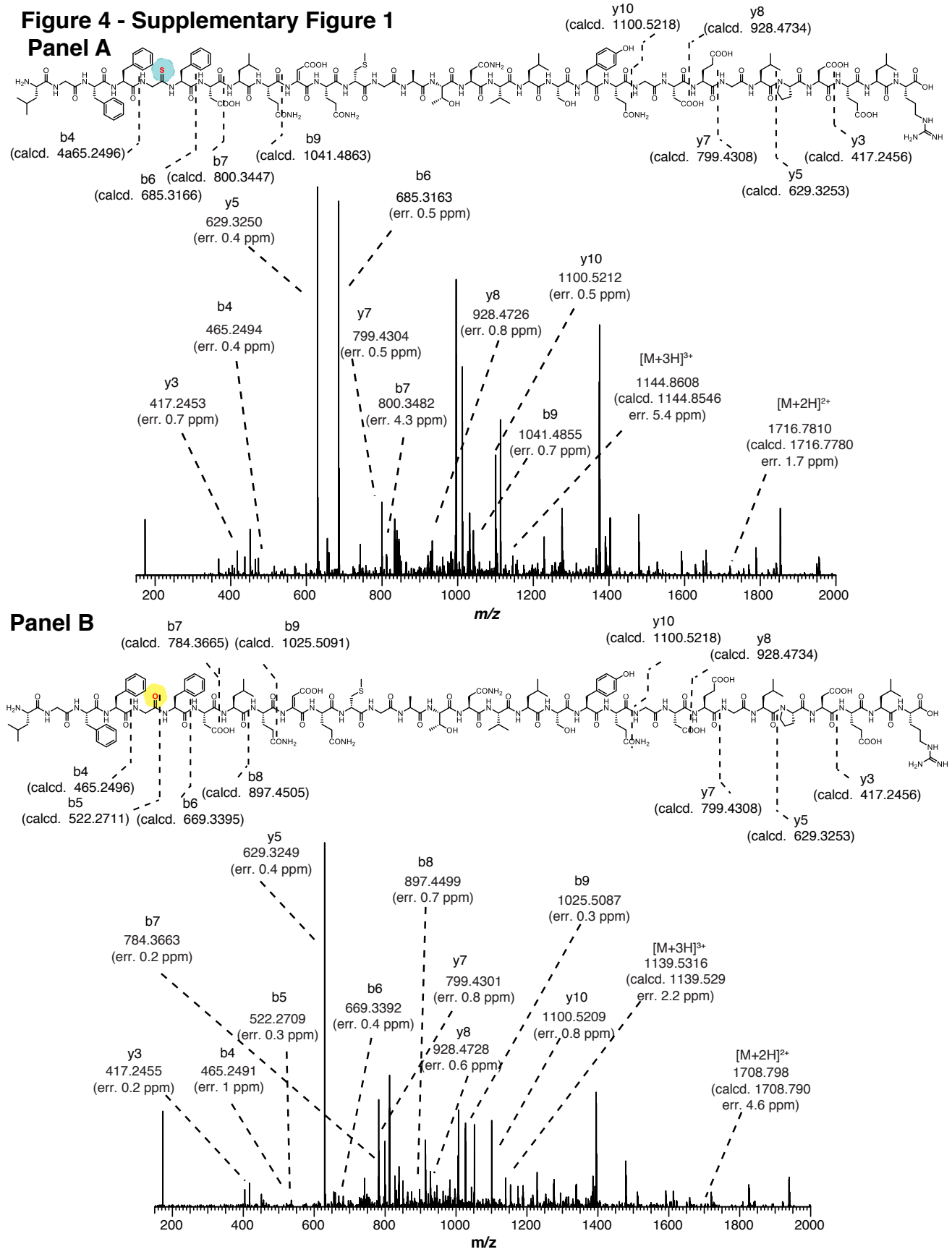

Fig. 4 - Supp. Fig 1: Panel A, High-resolutions electrospray ionization tandem mass spectrometry (HR-ESI MS/MS) analysis of a wild-type tryptic peptide from *Methanosarcina acetivorans* McrA (L461-R491, m/z 3432 Da). The b6 ion localizes the thioamide modification to Gly465. No b5 ion was detected suggesting negligible fragmentation at the thioamide bond. Predicted masses and associated errors are shown. **Panel B,** HR-ESI-MS/MS analysis of the corresponding McrA tryptic peptide from the Δ*ycaO-tfuA* deletion strain of *M. acetivorans* (m/z 3416 Da). The b5 and b6 ion localizes the amide functionality at Gly465. Predicted masses and associated errors are shown.

Figure 4 - Supplementary Figure 2

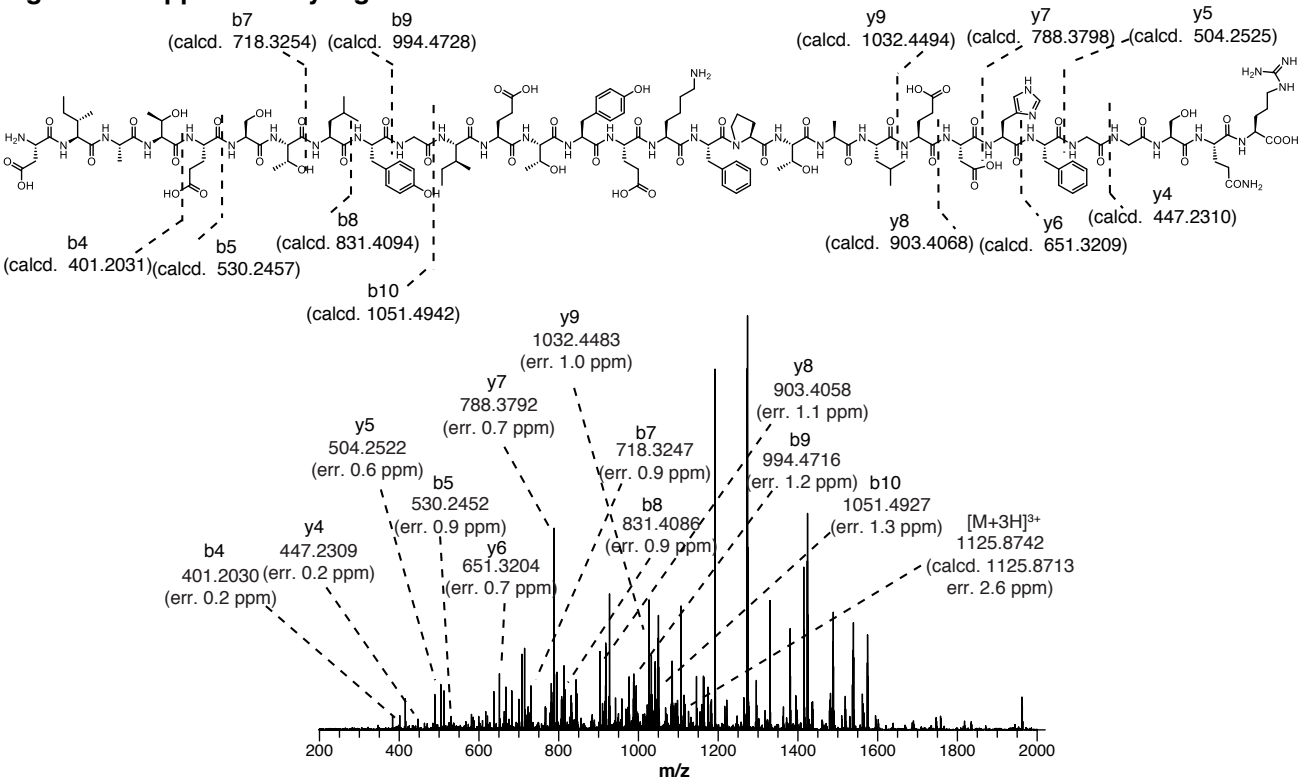

Fig. 4 - Supp. Fig. 2: HR-ESI-MS/MS of the tryptic peptide from *Methanosarcina acetivorans* McrA (D392-R421, m/z 3375 Da) present in both the wild-type and Δ*ycaO-tfuA* deletion strain. Predicted masses and associated errors are shown.

Figure 4 - Supplementary Figure 3

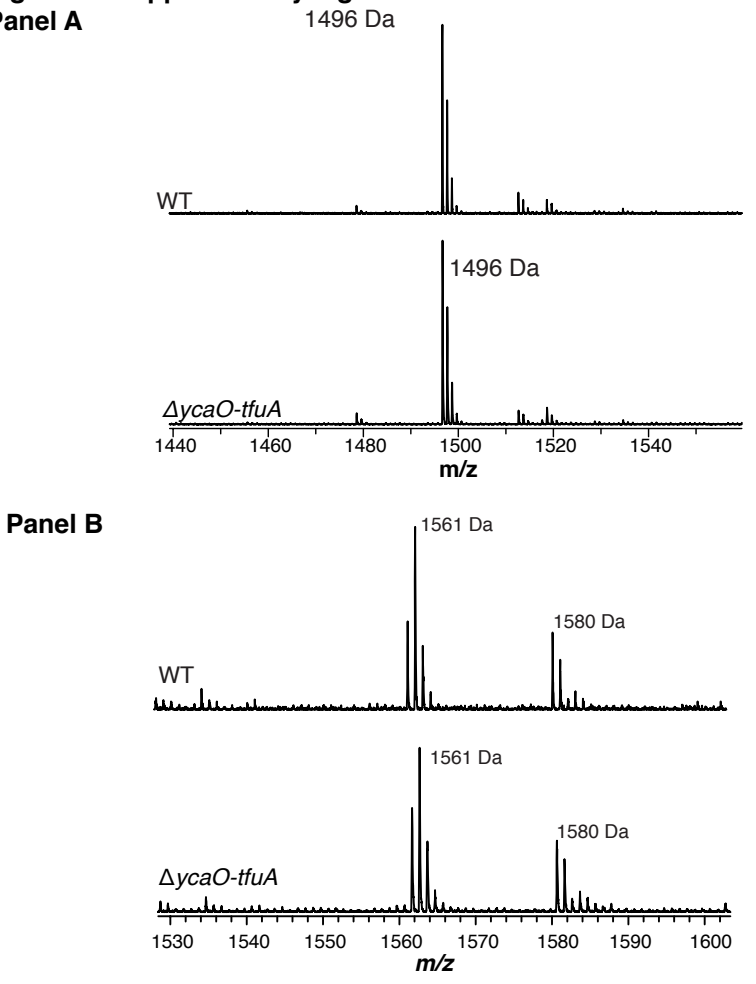

Fig. 4 - Supp. Fig. 3: Panel A, Matrix-assisted laser desorption/ionization time-of-flight mass spectrometry (MALDI-TOF MS) analysis of the wild-type (WT, top) and Δ*ycaO-tfuA* deletion strain (bottom) spectra identify the McrA tryptic peptide, H271-R284 (m/z 1496 Da), containing the known *N*-methylhistidine modification. This suggests that the thioglycine formation is not a prerequisite for this methylation event. **Panel B,** MALDI-TOF MS analysis of the WT (top) and Δ*ycaO-tfuA* deletion strain (bottom) spectra identify the McrA tryptic peptide, F408-R421, (m/z 1561 Da). This peptide has been reported to contain a β-methylation at Q420 in other methanogens (9), however, it remains unmodified in *M. acetivorans*.

Figure 5 - Supplementary Figure 1

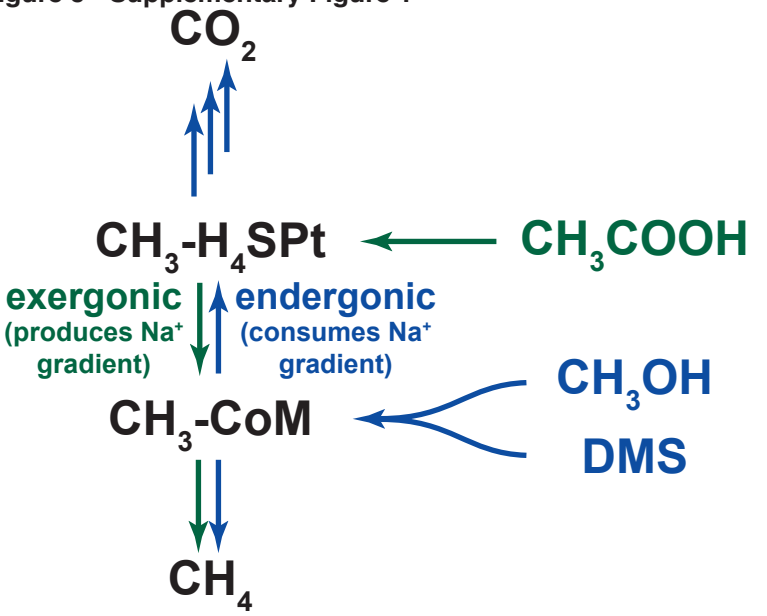

Fig. 5 - Supp. Fig. 1: An overview of methanogenic metabolism in *M. acetivorans*. Methylotrophic substrates such as methanol (CH_3OH) or dimethylsulfide (DMS) enter the methanogenic pathway via methylation of coenzyme M (CoM) and subsequent disproportionation to methane (CH_4) and carbon dioxide (CO_2; metabolic flux is shown as blue arrows). Notably, the first step in oxidation of CH_3-CoM to CO_2 is the energy-requiring transfer of the methyl moiety to generate methyl-tetrahydrosarcinapterin (CH_3-H_4SPt). In contrast, acetic acid enters the pathway at the CH_3-H_4SPt level, followed by reduction to CH_4 (green arrows). Thus, the second step of the pathway is exergonic.